Journal Pre-proofs

Polymeric micelles for cutaneous delivery of the hedgehog pathway inhibitor TAK-441: formulation development and cutaneous biodistribution in porcine and human skin

Aditya R. Darade, Maria Lapteva, Vincent Ling, Yogeshvar N. Kalia

PII: S0378-5173(23)00769-X
DOI: https://doi.org/10.1016/j.ijpharm.2023.123349
Reference: IJP 123349

To appear in: *International Journal of Pharmaceutics*

Received Date: 10 July 2023
Revised Date: 21 August 2023
Accepted Date: 23 August 2023

Please cite this article as: A. R. Darade, M. Lapteva, V. Ling, Y. N. Kalia, Polymeric micelles for cutaneous delivery of the hedgehog pathway inhibitor TAK-441: formulation development and cutaneous biodistribution in porcine and human skin, *International Journal of Pharmaceutics* (2023), doi: https://doi.org/10.1016/j.ijpharm.2023.123349

Polymeric micelles for cutaneous delivery of the hedgehog pathway inhibitor TAK-441: formulation development and cutaneous biodistribution in porcine and human skin

Aditya R. Darade[a,b], Maria Lapteva[a,b], Vincent Ling[c], Yogeshvar N. Kalia[a,b*]

[a] School of Pharmaceutical Sciences, University of Geneva, CMU, 1 rue Michel-Servet, 1211, Geneva 4, Switzerland

[b] Institute of Pharmaceutical Sciences Western Switzerland, University of Geneva, Geneva, Switzerland

[c] Takeda Pharmaceuticals, Drug Delivery Technologies Search and Evaluation, 40 Landsdowne St, Cambridge MA 02139

Corresponding author

Prof. Yogeshvar N. Kalia

School of Pharmaceutical Sciences, University of Geneva

CMU, 1 rue Michel-Servet, 1211, Geneva 4, Switzerland

Tel (dir): +41 (0)22 379 3355

Email: yogi.kalia@unige.ch

Abstract

TAK-441 is a potent inhibitor of the hedgehog pathway (IC_{50} 4.4 nM) developed for the treatment of basal cell carcinoma that is active against the vismodegib-resistant Smoothened receptor D473H mutant. The objective of this study was to develop a micelle-based formulation of TAK-441 using D-α-Tocopherol polyethylene glycol 1000 succinate (TPGS) and to investigate its cutaneous delivery and biodistribution. The micelles were prepared using solvent evaporation and incorporation of TAK-441 in the TPGS micelles increased aqueous solubility ~40-fold. The optimal formulation, a 3% HPMC hydrogel of TAK-441 loaded TPGS micelles, retained ~92% of the initial TAK-441 content (2.5 $mg_{TAK-441}/g$) after storage at 4 °C for 6 months. Finite dose experiments using human skin demonstrated that this formulation resulted in significantly greater cutaneous deposition of TAK-441 after 12 h than a non-micelle control formulation, (0.40 ± 0.11 $\mu g/cm^2$ and 0.05 ± 0.02 $\mu g/cm^2$, respectively) – no transdermal permeation was observed. The cutaneous biodistribution profile demonstrated that TAK-441 was predominantly delivered to the viable epidermis and upper dermis. Delivery from the HPMC hydrogel formulation resulted in TAK-441 epidermal concentrations that were several thousand-fold higher than the IC_{50}, with almost negligible transdermal permeation, thereby decreasing the risk of systemic side effects *in vivo*.

Keywords: Basal cell carcinoma, TAK-441, skin, topical delivery, D-α-tocopherol polyethylene glycol succinate, polymeric micelles, biodistribution

Abbreviations

AE	Adverse effects
BCC	Basal cell carcinoma
BSA	Bovine serum albumin
cAMP	Cyclic adenosine monophosphate
DPBS	Dulbecco's phosphate-buffered saline
GLI	Glioma-associated oncogenes homologue
GPR161	G-Protein coupled receptor 161
HH	Hedgehog

HPC	Hydroxypropyl cellulose
HPMC	Hydroxypropylmethylcellulose
KIF7	Kinesin Family Member 7 Protein
LOD	Limit of detection
LOQ	Limit of quantification
MFD	Maximum feasible dose
NR	Nile red
p53	Tumor suppressor protein p53
PC	Primary cilium
P.D.I.	Polydispersity index
PKA	Protein kinase A
PTCH1	Patched 1 Protein
SMO	Smoothened receptor
SUFU	Suppressor of Fused homolog
TEM	Transmission electron microscopy
TPGS	D-α-Tocopherol polyethylene glycol 1000 succinate
UHPLC	Ultra-high performance liquid chromatography

UV Ultraviolet

1. Introduction

Basal cell carcinoma (BCC) is one of the most common cancers in the world constituting approximately 90% of all skin cancers with an incidence of 100 in 100,000 in the UK and 884 in 100,000 in Australia (Madan et al., 2010; Staples et al., 2006). The major causative factor is UV light (Couvé-Privat et al., 2002; Daya-Grosjean and Sarasin, 2000); UV-B damage causes C to T (or CC to TT) structural mutations in the DNA of epidermal basal cells (Athar et al., 2006).

The hedgehog (HH) signaling pathway is highly active during embryonic development but is inactive in most adult tissues except to maintain stem cell populations and to regulate the growth of hair follicles and sebaceous glands (Athar et al., 2006) – however, it is prominently involved in the progression of BCC. Mutations in the Patched 1 (PTCH1) and Smoothened (SMO) proteins lead to a loss of function in PTCH1 or gain of function in SMO. This can lead to activation of the GLI family of transcription factors (Dlugosz et al., 2012) resulting in the hyperproliferation of basal cells seen in BCC (Roewert-Huber et al., 2007; Samarasinghe and Madan, 2012). Inactivation of PTCH1 has been proposed to be a necessary step in progression of BCC (Gailani and Bale, 1997).

Locally advanced BCC patients are not eligible for surgery or radiotherapy (Gould et al., 2014). As a result, pharmacotherapies involving the inhibition of SMO and hence preventing activation of the HH signaling pathway have been developed. Vismodegib is a “first-in-class” synthetic inhibitor of SMO (Robarge et al., 2009; Gould et al., 2014), which was approved by the US Food and Drug administration (FDA) for the treatment of metastatic or locally advanced BCC in 2012 (Dlugosz et al., 2012). Sonidegib, another hedgehog inhibitor, was approved by the US FDA for the treatment of locally advanced BCC in 2015 (Burness, 2015). However, mutations in SMO can inhibit its interaction with such drugs, resulting in resistance to the treatment. The first cases describing acquired resistance to vismodegib treatment due to mutation in SMO (SMO-D473H) were reported in 2009 – i.e. even before the approval of vismodegib in 2012 (Yauch et al., 2009). Treatment with sonidegib in patients with resistance to vismodegib was ineffective (Jain et al., 2017). Furthermore, resistance to treatment with sonidegib, due to mutations in the drug binding site of SMO (SMO-D473 and SMO-Q477), has also been reported (Danial et al., 2016; Jain et al., 2017; Nguyen and Cho, 2022).

TAK-441 is a potent inhibitor of the HH pathway (IC_{50} 4.4 nM; determined by luciferase reporter activities in NIH3T3 cells carrying a stably transfected GLI-reporter construct) and is effective against vismodegib-resistant SMO mutant D473H (Goldman et al., 2015; Ishii et al., 2014; Ohashi et al., 2012). Ishii et al. reported TAK-441 as having an IC_{50} of 79 nM in D473H-transfected cells; in comparison, the IC_{50} of vismodegib was 7100 nM.

TAK-441 has a molecular weight of 576.57 Da (**Figure 1**), is moderately lipophilic (log P 2.61) but has very poor aqueous solubility (81 µg/mL at pH 6.8) (Ohashi et al., 2012; Ishii et al., 2014). Phase I clinical trials have investigated its oral administration at doses ranging from 50 mg/day up to a maximum feasible dose (MFD) of 1600 mg/day (Goldman et al., 2015). GLI1 expression in skin biopsies was strongly inhibited at all doses but there were various side effects. All patients experienced at least one adverse effect (AE); mild to moderate AE were dysgeusia, fatigue, nausea, muscle spasm, hyponatremia and fatigue (Goldman et al., 2015). Approximately 35% of patients experienced serious AE including gastrointestinal disorders, neoplasms (progression of underlying disease), and hepatobiliary disorders.

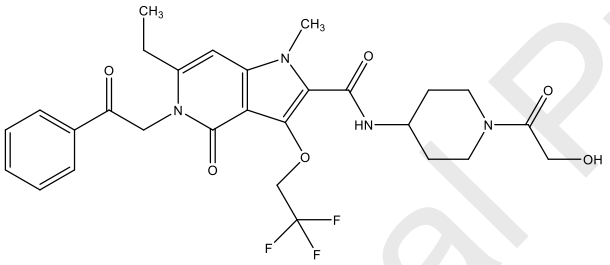

Figure 1. Chemical structure of TAK-441 (MW 576.57 Da; log P 2.61; aqueous solubility 81 µg/mL at pH 6.8)

Topical delivery of TAK-441 could not only improve the efficacy through better targeting the site of disease but also increase treatment tolerability by reducing systemic side effects. Direct application to the disease site obviously lowers the dose required as compared to oral administration and by definition reduces systemic or "off-target" toxicity. However, topical pharmacotherapy using TAK-441 must ensure sufficient cutaneous bioavailability and more specifically that supra-therapeutic concentrations are achieved in the basal epidermis. An interesting preclinical study evaluating the activity of a panel of SMO inhibitors using both cell-based assays and a mouse model concluded that LEQ-506 and TAK-441 might be suitable for topical application and local treatment of BCC (Lauressergues et al., 2016). Given the poor aqueous solubility of the SMO inhibitors, the vehicles used for the topical delivery studies comprised either (i) propylene glycol 60% (v/v) / DMSO 40% (v/v) or (ii) propylene glycol 70%

(v/v) / DMSO 20% (v/v) / EtOH 10% (v/v). However, these formulations would obviously not be suited for clinical applications. Although it is simpler to formulate TAK-441 in a more lipophilic system where it is more soluble, the greater solubility and hence formulation stability comes at the expense of a lower thermodynamic activity and less favorable partitioning into the stratum corneum.

Polymeric micelles are colloidal nanocarriers formed from polymeric surfactants that self-assemble in aqueous media at concentrations above the critical micelle concentration (Lavasanifar et al., 2002). We have previously described how methoxypoly(ethylene glycol)-di-hexyl-substituted-poly(lactic acid) (mPEGhexPLA) micelles can be used to develop aqueous formulations of several poorly water soluble therapeutics with dermatological applications: econazole (Bachhav et al., 2011), tacrolimus (Lapteva et al., 2014a), ciclosporin (Lapteva et al., 2014b), retinoic acid (Lapteva et al., 2015), imiquimoid (Lapteva et al., 2019) and spironolactone (Dahmana et al., 2021) and enable their improved cutaneous delivery as compared to existing approved formulations (Lapteva et al., 2014a, 2015, 2019). Furthermore, in another study, mPEGhexPLA micelles were used to develop the first topical formulation of vismodegib and the cutaneous biodistribution method used to show that therapeutically relevant amounts of drug could be delivered into the epidermis and upper dermis (Kandekar et al., 2019).

In other studies we have used D-α-tocopherol polyethylene glycol succinate 1000 (TPGS) as the copolymer to solubilize adapalene (Kandekar et al., 2018), sirolimus (Quartier et al., 2021a) and to co-formulate econazole, terbinafine and amorolfine (Gou et al., 2022). This biocompatible and biodegradable surfactant is an amphiphilic derivative of natural vitamin E that has been approved by the regulatory authorities as an excipient for pharmaceutical products (Aggarwal et al., 2012). It has been approved by the US FDA as a pharmaceutical ingredient and has been used as an excipient in various marketed products (Zhang et al., 2015; Vadlapudi et al., 2014). TPGS was approved by the European Medicines Agency in 2009 as an API (active pharmaceutical ingredient; Vendrop®), for the treatment of vitamin E deficiency due to digestive malabsorption in pediatric patients suffering from congenital chronic cholestasis or hereditary chronic cholestasis (Papas, 2021).

The objectives of the present study were (i) to investigate the feasibility of using TPGS micelles to overcome the intrinsic poor aqueous solubility of TAK-441 and to develop a stable aqueous formulation, (ii) to characterize the micelles in terms of drug content, size, and morphology, (iii) to develop a user-friendly micelle-based hydrogel formulation for topical application and to determine its stability, (iv) to study the cutaneous delivery of TAK-441 and to determine the cutaneous biodistribution in porcine skin after application of micelle solution and micelle-based hydrogel formulations and to compare the results to those obtained with a non-micelle control formulation, and (v) to confirm the results using human skin.

2. Materials and Methods

2.1 Materials

TAK-441 was kindly provided by Takeda Pharmaceutical Company Ltd, Japan. D-α-Tocopherol polyethylene glycol 1000 succinate (TPGS), formic acid (MS grade), isopentane, and Dulbecco's phosphate-buffered saline (DPBS), hydroxypropyl methylcellulose (HPMC, ~26 kDa; methoxyl content 19-24 % and hydroxypropoxyl content 7-12 %) were purchased from Sigma-Aldrich (Buchs, Switzerland). Low molecular weight HPMC – Methocel™ E5 Premium LV (~10 kDa; methoxyl content 28-30 % and hydroxypropoxyl content 7-12 %) was procured from Dow Chemicals (Horgen, Switzerland). Hydroxypropyl cellulose (Klucel™ MF Pharm, HPC; M.W. ~ 850 kDa) and glycerol were purchased from Hänseler AG (Herisau, Switzerland). Bovine serum albumin (BSA) was purchased from Axon Lab (Baden-Dättwil, Switzerland). Acetone (analytical grade) and Nile Red dye were obtained from Acros Organics (Geel, Belgium). Methanol and acetonitrile (LC-MS grade) were purchased from Fisher Scientific (Reinach, Switzerland). PTFE membrane filters (0.22 µm), Amicon Ultra 0.5 mL (5 kDa) filtration units were purchased from VWR (Nyon, Switzerland). Ultrapure water (Millipore Milli-Q Gard 1 Purification Pack resistivity >18 MΩ.cm; Zug, Switzerland) was used for formulation development and analysis. All other chemicals were at least of analytical grade.

2.2 Analytical methods

TAK-441 was quantified using a Waters Acquity Core UPLC® system equipped with a Xevo® TQ-MS tandem quadrupole detector. Isocratic separation was performed using an Acquity UPLC® BEH C18 column (2.1 x 50 mm; 1.7 µm) in tandem with an Acquity UPLC® C18 VanGuard pre-column (2.1 x 5 mm, 1.7 µm) that was maintained at 25 °C. The mobile phase consisted of a mixture of acetonitrile and water (75:25 v/v). The flow rate and injection volume were 0.1 mL/min and 5 µL, respectively. The TAK-441 peak was observed at 1.7 min, and the run time was 3.0 min. Mass spectrometric detection was performed with electrospray ionization in positive ion mode using multiple reaction monitoring (MRM). The detection settings for TAK-441 are presented in **Table 1**. The limits of detection (LOD) and quantification (LOQ) were 1.29 and 3.29 ng/mL, respectively. The UHPLC-MS/MS method was validated as per ICH guidelines (complete details are provided in the **Supplementary Data, Section 1**).

Table 1: MS/MS Settings for the detection of TAK-441

	TAK-441
Nature of parent ion	Hydrogen adduct $[M + H]^+$
Parent ion (m/z)	577.40
Daughter ions (m/z)	419.26

Collision energy (V)	32
Cone voltage (V)	36
Capillary voltage (kV)	2.9
Desolvation temperature (°C)	350
Desolvation gas flow (L/h)	650
Cone gas flow (L/h)	2
Collision gas flow (mL/min)	0.15
LM resolution 1	2.96
HM resolution 1	15
Ion energy 1 (V)	0.3
LM resolution 2	2.91
HM resolution 2	15.24
Ion energy 2 (V)	0.6

2.3 Preparation of micelle formulations

Micelle solution: The TPGS micelles containing TAK-441 were prepared by the solvent evaporation method (Kandekar et al., 2019). The screening of surfactants and their concentration was done using a micro-scale formulation technique that enables multiple simultaneous experiments with minimal amounts of drug and excipients. This reduces the material cost, the time

required for excipient screening and formulation development as well as decreasing exposure to the drug, which is beneficial when working with cytotoxic compounds. Short-listed formulations were then scaled up to lab-scale batches. Briefly, the known amounts of TPGS and TAK-441 were dissolved in 2 mL of acetone to obtain a clear solution. This solution was added slowly to 4 mL water under sonication (Branson Digital Sonifier S-450D). Acetone was then slowly removed by using a rotary evaporator (Büchi RE 121 Rotavapor). The final volume was made up with water in a volumetric flask to obtain the micelle formulation with TAK-441 and TPGS concentrations of 3 mg/mL and 10 mg/mL, respectively. After equilibration overnight, the micelle solution was centrifuged at 10,000 rpm for 15 min (Eppendorf Centrifuge 5804) to remove excess TAK-441, and the supernatant was carefully collected.

Micelle gels: In preliminary studies, TAK-441-TPGS micelles were incorporated into a 3% HPC gel to study the cutaneous delivery of TAK-441 from a semi-solid gel formulation. The formulation was compared with the control gel having the same composition except for the polymeric surfactant. Based on the preliminary results, it was decided to prepare a micelle-based HPMC gel with better formulation properties for clinical application (see below for complete details; section 3.1).

2.4 Characterization of micelle formulations

Size determination: The hydrodynamic diameter (Z_{av}), polydispersity index (P.D.I.), and volume weighted and number weighted diameters (d_v and d_n, respectively) of the micelles were measured using dynamic light scattering (DLS) with a Zetasizer HS 3000 (Malvern Instruments Ltd.; Malvern, UK). Measurements were performed at an angle of 90° and a temperature of 25 °C. All values were obtained after 3 runs of 10 measurements.

Morphology: Micelle morphology was characterized with transmission electron microscopy (TEM) (FEI Tecnai G2 Sphera, Eindhoven, Netherlands) using the negative staining method. Briefly, 5 μL of the micelle solution was dropped onto an ionized carbon-coated copper grid (0.3 Torr, 400 V for 20 s). The grid was then placed for 1 s in a 100 μL drop of a saturated uranyl acetate aqueous solution and then in a second 100 μL drop for 30 s. The excess staining solution was removed, and the grid was dried at room temperature before the measurement.

Determination of TAK-441 content in the micelles: TAK-441 loaded into the micelles was quantified by UHPLC-MS/MS. To ensure complete micelle destruction and release of the incorporated drug, formulations were diluted in acetonitrile and analyzed. The drug content, drug loading, and entrapment efficiency were calculated using equations 1−3:

$$Drug\ content\ \left(\frac{mg}{mL}\right) = \frac{Drug\ in\ the\ formulation\ (mg)}{Volume\ of\ the\ formulation\ (mL)} \quad (1)$$

$$Drug\ loading\ \left(\frac{mg\ of\ drug}{g\ of\ polymer}\right) = \frac{Drug\ in\ the\ formulation\ (mg/mL)}{Polymer\ in\ the\ formulation\ (g/mL)} \quad (2)$$

$$Entrapment\ efficiency\ (\%) = \frac{Drug\ entrapped\ in\ micelles\ (mg)}{Drug\ added\ (mg)} \times 100 \quad (3)$$

Viscosity measurements: The viscosity of the micelle gels was measured by using a Thermo Scientific™ HAAKE™ MARS™ rheometer. The measurements were carried out at 25 °C using a rotating plate spindle at different shear rates. The measurements and post-measurement evaluations were carried out using Thermo Scientific™ HAAKE™ RheoWin software.

Evaluation of micelle formulation stability: The TAK-441 micelle aqueous formulation and micelle-based HPMC gel formulation were prepared and stored at 4 °C for 6 months. The formulations were assayed to determine drug content at various time points (day 1, followed by time points at monthly intervals).

2.5 Cutaneous delivery and biodistribution studies *in vitro*

2.5.1 Skin preparation

Porcine ears were purchased from a local abattoir (CARRE; Rolle, Switzerland) shortly after sacrifice. After washing under running cold water, skin samples with a thickness of ~0.8 mm were carefully harvested from the outer region of the ear using a Zimmer air dermatome (Münsingen, Switzerland). Hair was removed from the skin surface using clippers. Discs corresponding to the permeation area were punched out (Berg & Schmid HK 500; Urdorf, Switzerland). Skin samples were frozen at −20 °C and stored for a maximum period of 3 months. Before the experiment, skin samples were thawed at room temperature and placed for 15 min in 0.9% saline solution for rehydration.

Human skin samples were obtained shortly after surgery from the Department of Plastic, Aesthetic and Reconstructive Surgery, Geneva University Hospital (Geneva, Switzerland), fatty tissue was removed and the skin was stored at −20 °C. The donation was approved by the Cantonal Commission for Ethics in Research (CCER 2021-01578).

2.5.2 Micelle solution

The experiments to determine cutaneous deposition and transdermal permeation were performed using standard two-compartment vertical (Franz-type) diffusion cells, (Milian SA; Meyrin, Switzerland) with a cross-sectional area of 2 cm^2. The receptor compartment contained 10 mL Dulbecco's phosphate-buffered saline (DPBS) pH 7.4 supplemented with 1% BSA to maintain sink conditions. The receiver compartment was maintained at 32-34 °C throughout the experiments. For infinite dose conditions, 200 µL of TAK-441 micelle solution (3 $mg_{TAK-441}$/mL) was applied to the skin sample surface (i.e. 300 µg of TAK-441/cm^2 of the skin surface) and for

finite dose studies, 20 µL of micelle solution (again, 3 mg $_{TAK-441}$/mL) was applied (30 µg/cm^2 of TAK-441/cm^2 of the skin surface). A non-micelle formulation comprised of 3 mg/mL TAK-441 suspended in aqueous 0.05% hydroxypropyl cellulose (HPC) was used as a control. TAK-441 had the least solubility in HPC (**Supplementary Data, Section 7**); this would minimize the risk of interference of the suspending agent on drug delivery. Aliquots (1 mL) were withdrawn from the receiver compartment at 1, 4, and 12 h and replaced with an equivalent volume of fresh media. Samples were diluted in acetonitrile to precipitate BSA. After centrifugation at 10,000 rpm for 15 min, the permeation samples were analyzed by UHPLC-MS/MS. Upon completion of the experiments, the excess formulation was removed from the skin surface using the validated wash method (**Supplementary Data, Section 4**). The skin samples were cut into small pieces, and TAK-441 deposited in the skin was extracted by soaking the pieces in 2 mL of methanol for 4 h with continuous stirring at room temperature. The extraction procedure was validated (**Supplementary Data, Section 3**). The extraction samples were centrifuged at 10,000 rpm for 15 min, diluted, and filtered through a 0.22 µm PTFE filter before UHPLC-MS/MS analysis. Filter adsorption studies were conducted to identify the appropriate filter (**Supplementary Data, Section 2**).

2.5.3 Micelle gel

TAK-441 micelles were incorporated into 3 % HPC gel to test the cutaneous delivery of TAK-441 to porcine skin from a semi-solid formulation. The composition of the control gel was the same except for the polymeric surfactant. The experiments were performed as described above (section 2.5.2). For infinite dose, 200 mg of micelle gel (2.88 mg$_{TAK-441}$/g of gel formulation; i.e. the gel contained 0.29 % TAK-441) was applied on the skin surface (i.e. 288 µg TAK-441/ cm^2 of the skin surface) and for finite dose, 20 mg of micelle gel was applied (28.8 µg/cm^2 TAK-441/ cm^2). Similar experimental conditions were used for the micelle-based HPMC gel, which was used to test delivery to human skin. For infinite dose, 200 mg of micelle gel (2.5 mg$_{TAK-441}$/g of gel formulation; i.e. the gel contained 0.25 % TAK-441) was applied on the skin surface (i.e. 250 µg TAK-441/ cm^2 of the skin surface) and for finite dose, 20 mg of micelle gel was applied (25 µg/cm^2 TAK-441/ cm^2). The composition of the control gel was the same as the HPMC gel except for the TPGS.

Upon completion of the experiment, a punch was used to separate the skin sample into two parts in order to determine the cutaneous deposition and cutaneous biodistribution of TAK-441 following application of the gel formulations an inner disk with a surface area of 0.785 cm^2 and a remaining outer ring with an area of 1.215 cm^2. This outer ring was subsequently cut into small pieces, and TAK-441 deposited in the tissue was extracted by the validated extraction method (section 2.5.2 and **Supplementary Data, Section 3**) followed by quantification using UHPLC-MS/MS. The 0.785 cm^2 disks that were punched out were used to determine the TAK-441 biodistribution as a function of depth in the skin. These skin discs were snap-frozen in isopentane cooled by liquid nitrogen. For this, the skin samples were fixed with O.C.T. on a circular piece of cork and a plastic o-ring placed around the skin discs to avoid tissue compression and to ensure a flat frozen sample. This ensured the integrity of the thickness of different regions of the skin. The skin discs were then cryosectioned (Thermo Scientific™ CryoStar™ NX70; Reinach, Switzerland) to obtain 50 µm thick sections starting from the stratum corneum surface down to a skin depth of 400 µm. These lamellae enabled the amounts of TAK-441 to be determined as a function of position in the skin, encompassing the stratum corneum, epidermis, and upper dermis,

respectively. Each lamella and the remaining dermis were individually extracted in 250 µL methanol for 4 h and TAK-441 was quantified by UHPLC-MS/MS.

2.6 Statistical analysis

Data were expressed as the mean ± SD. Outliers determined using the Grubbs test were discarded. Results were evaluated statistically using analysis of variance (ANOVA) one-way followed by the Tukey test for multiple comparisons or Student's t test. The level of significance was fixed at $\alpha = 0.05$.

3. Results and Discussion

3.1 Micelle formulation development and characterization

A set of formulations (A-H) were prepared with constant TPGS content (10 mg/mL) but different target TAK-441 loadings: 100, 150, 200, 250, 300, 350, 400 and 500 mg of TAK-441 per g of TPGS. The drug loadings, drug contents, and incorporation efficiencies obtained for each formulation are given in **Table 2**. The highest drug content was provided by Formulation E (2.97 ± 0.071 mg/mL).

Table 2: Micelle formulation characterization with respect to drug content and size

Formulation	TPGS content (mg/mL)	Target loading ($mg_{TAK-441}/g_{TPGS}$)	Drug content			Size			
			Drug loading ± SD ($mg_{TAK-441}/g_{TPGS}$)	Drug content ± SD ($mg_{TAK-441}/mL_{formulation}$)	Entrapment efficiency ± SD (%)	Z_{av} (nm)	P.D.I.	d_v (nm)	d_n (nm)
A	10	100	98.41 ± 1.87	0.98 ± 0.018	98.41 ± 1.87	14.01	0.063	12.29	10.45
B	10	150	147.21 ± 2.29	1.47 ± 0.023	98.14 ± 1.53	14.45	0.176	11.72	9.71

C	10	200	199.22 ± 3.86	1.99 ± 0.038	99.61 ± 1.93	13.83	0.071	11.79	9.39
D	10	250	239.50 ± 6.78	2.39 ± 0.068	95.80 ± 2.71	14.24	0.172	11.78	9.76
E	10	300	297.18 ± 7.08	2.97 ± 0.071	99.06 ± 2.36	14.33	0.172	11.32	9.86
F	10	350	216.34 ± 31.95	2.16 ± 0.320	61.81 ± 9.13	12.14	0.309	10.55	8.74
G	10	400	197.40 ± 28.56	1.97 ± 0.286	49.35 ± 7.14	16.92	0.306	12.07	10.51
H	10	500	207.35 ± 28.45	2.07 ± 0.285	41.47 ± 5.69	16.90	0.305	11.86	9.91

Size characterization: TAK-441 loaded TPGS micelles were characterized to determine their size using DLS (**Table 2**). All TAK-441 loaded micelle formulations presented uniform nanometer sizes with hydrodynamic diameters (Z_{av}) from 12.14 to 16.92 nm. The volume weighted diameter (d_v) measurements ranged from 10.55 to 12.29 nm and the number weighted diameter (d_n) ranged from 8.74 to 10.51 nm. A TEM micrograph of the optimized formulation (Formulation E) is shown in **Figure 2** where it is apparent that the micelles were spherical in shape with diameters ranging from 10 to 15 nm; these dimensions were consistent with those from DLS (**Table 2**).

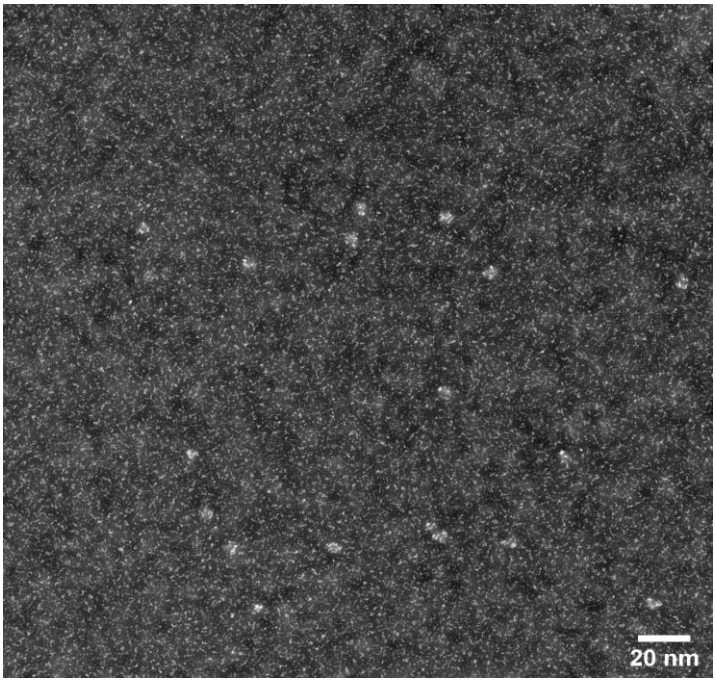

Figure 2. TEM image of TAK-441 loaded TPGS micelles present in Formulation E (at a nominal 3 $mg_{TAK\text{-}441}/mL_{formulation}$)

Development of HPC micelle gel: Formulation E was used to prepare a 3 % HPC gel having a final drug content of 2.88 $mg_{TAK\text{-}441}$/g of gel formulation. The viscosity of the gel was 283.5 Pas at a shear rate of 0.01 s^{-1} (**Figure 3**). As mentioned above, a 3% HPC gel with TAK-441 was used as the control – this would ensure that any superiority in skin delivery of TAK-441 from the micelle gel would be specifically due to the effect of encapsulation in the micelles.

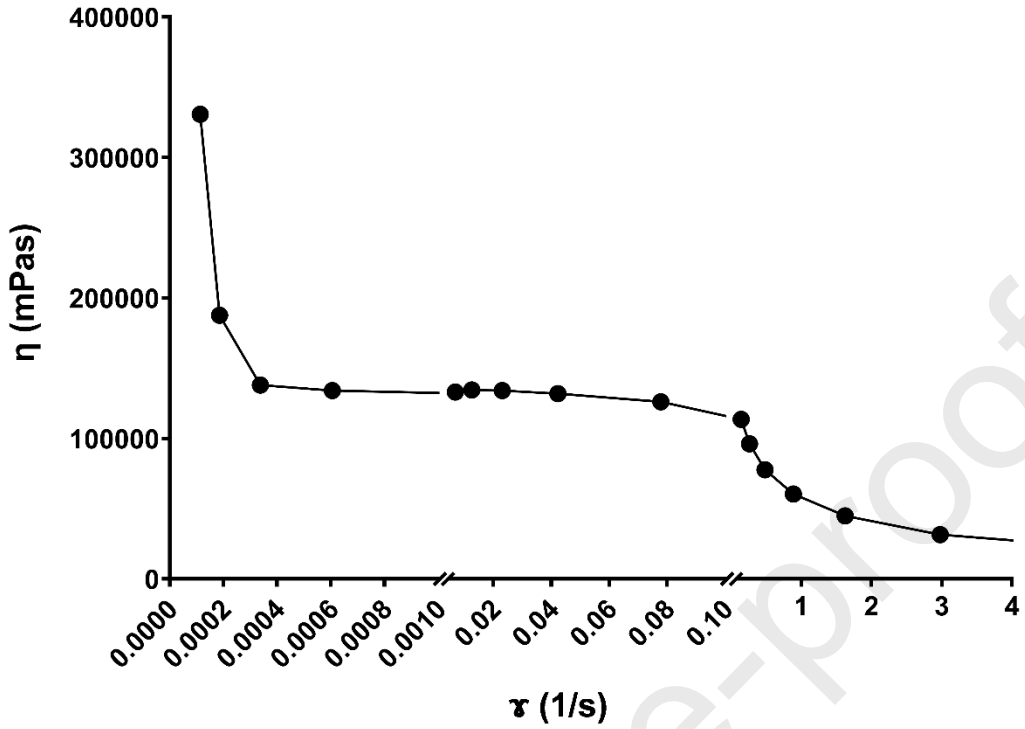

Figure 3. Rheogram of TAK-441 loaded TPGS micelle-based 3 % HPC gel.

3.2 Evaluation of TAK-441 delivery in porcine skin *in vitro*

3.2.1 Cutaneous delivery of TAK-441 from micelle solution

This study was performed to compare the cutaneous deposition and transdermal permeation of TAK-441 from the TPGS micelle solution and a control formulation. In these initial experiments, porcine skin was used to investigate TAK-441 delivery as it is one of the best surrogates for human skin (Dick and Scott, 1992; Schmook et al., 2001; Herkenne et al., 2006; Jacobi et al., 2007). The concentration of TAK-441 present in the receiver compartment was below the LOD of the UHPLC-MS/MS method – corresponding to a cumulative permeation of < 0.1 pg/cm^2 after formulation application for 12 h. As shown in **Figure 4A**, higher skin deposition was observed with the micelle solution groups (infinite and finite dose) than with the control formulation. The amount of TAK-441 deposited in porcine skin from the micelle solution and control formulation under infinite dose conditions was 1.44 ± 0.27 µg/cm^2 and 0.41 ± 0.09 µg/cm^2 (p=0.015, one-way ANOVA; n = 6) and that for finite dose was found to be 0.61 ± 0.11 µg/cm^2 and 0.19 ± 0.052 µg/cm^2 (p=0.029, one-way ANOVA; n = 6), respectively. Under infinite dose conditions, the concentration corresponding to the total amount of TAK-441 deposited in the whole skin sample after application of the micelle solution was >7,100-fold than its IC_{50} of 4.4 nM (Ohashi et al., 2012), and that at finite dose was >3,000-fold higher.

3.2.2 Cutaneous delivery of TAK-441 from the micelle-HPC gel

The amount of TAK-441 deposited in porcine skin after application of the micelle HPC gel and control HPC gel formulation under infinite dose conditions was 0.74 ± 0.19 µg/cm^2 and 0.12 ± 0.05 µg/cm^2 (p=0.002, one-way ANOVA; n = 6) and that for finite dose was 0.32 ± 0.08 µg/cm^2 and 0.03 ± 0.01 µg/cm^2 (p=0.002, one-way ANOVA; n = 6), respectively. Thus, the concentration of TAK-441 quantified in skin samples after 12 h of delivery was significantly higher in micelle treated groups (solution and gel) as compared to control formulations in porcine skin.

The biodistribution studies enabled the amounts of TAK-441 deposited in the skin to be determined as a function of depth. Biodistribution at infinite and finite dose revealed that greater amounts of TAK-441 were predominantly present at the target tissue layer, i.e. the epidermal region (**Figure 4B and 4C**). Given the amounts of TAK-441 present in these smaller skin volumes, the estimated concentrations, were higher than those estimated for the skin sample as a whole. Hence, in the first lamella, going from 0 to 50 µm, the TAK-441 concentration achieved after application of the micelle-HPC gel at infinite and finite dose was >14,000-fold and >7,500-fold higher, respectively, than the IC_{50} ; whereas, for the 50-100 µm region, the corresponding values were >6,800-fold and >3,400- fold higher, respectively.

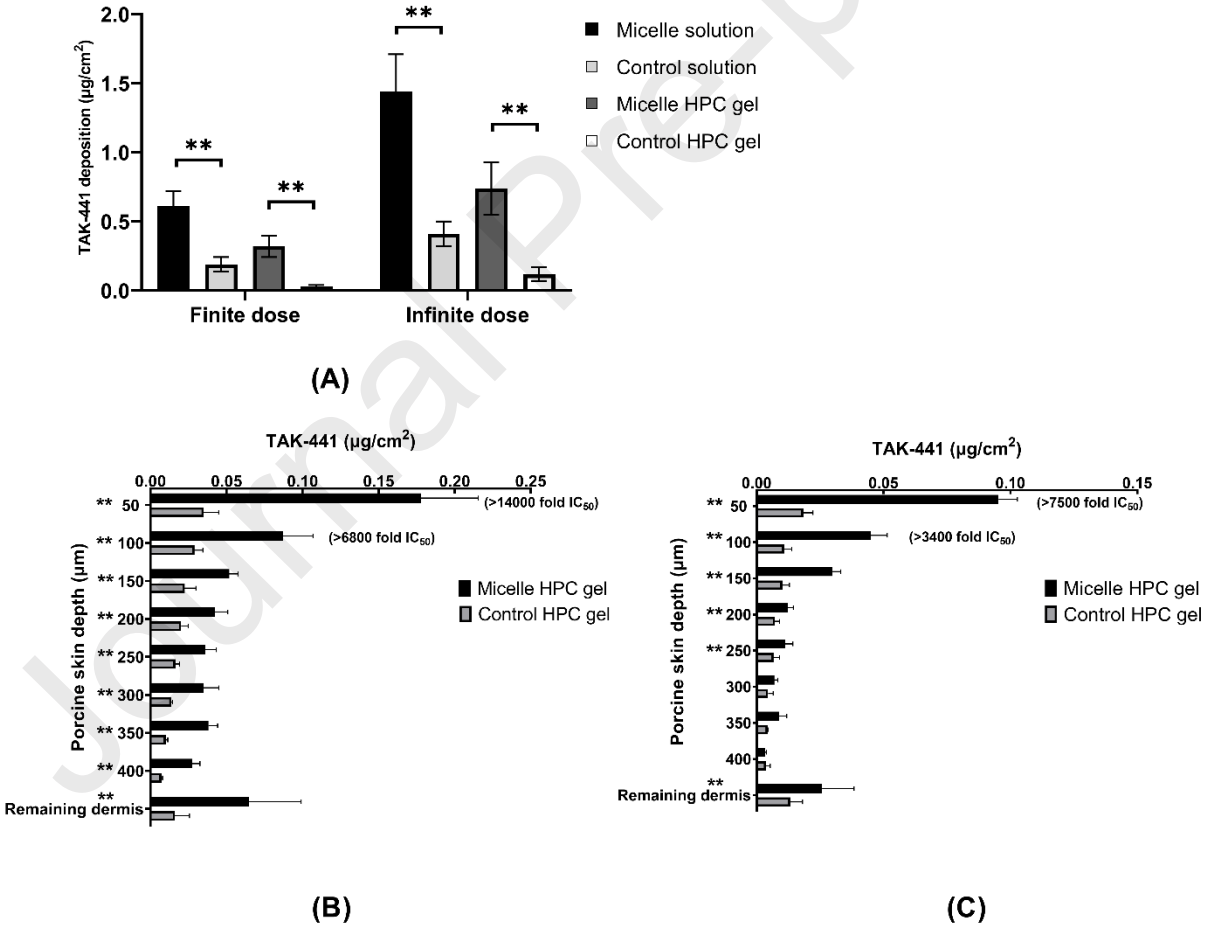

Figure 4. Cutaneous deposition and biodistribution of TAK-441 in porcine skin (micelle solution and micelle HPC gel formulation, n = 6). (**A**) Cutaneous deposition of TAK-441, (**B**) Cutaneous

biodistribution of TAK-441 at infinite dose, and (**C**) Cutaneous biodistribution of TAK-441 at finite dose; (**P < 0.05, one-way ANOVA). (Mean ± SD)

3.3 Cutaneous delivery of TAK-441 using micelle-HPMC gel in human skin

3.3.1 Development of a micelle-HPMC gel

After the promising results obtained using porcine skin, it was decided to perform cutaneous delivery studies using a micelle gel formulation of TAK-441 and human skin. However, since HPC precipitates at relatively low temperatures (cloud point: ~39 °C) and given that this could cause stability problems (Greiderer et al., 2011), it was decided to develop a HPMC-based micelle gel formulation (**Table 3**). The drug content of the HPMC-based gels was slightly lower than that used previously – 2.5 $mg_{TAK-441}$/g of gel formulation. The viscosity of the gel was found to be 646.9 Pas at a shear rate of 0.01 s^{-1} (**Figure 5**) with shear-thinning behavior that would be advantageous for the ease of application due to its better spreadability (Brummer and Godersky, 1999; Kwak et al., 2015).

Table 3. TAK-441-TPGS micelle-based HPMC gel composition

Component	Concentration (% w/w)	Role
TAK-441	0.25	Investigational molecule
TPGS	0.93	Micelle forming agent
HPMC	5	Gel base
Methocel™ E5 Premium LV	3	Gel base
Glycerol	2	Rheology modifier
Sodium metabisulfite	0.1	Preservative
Water	Q.S.	Vehicle

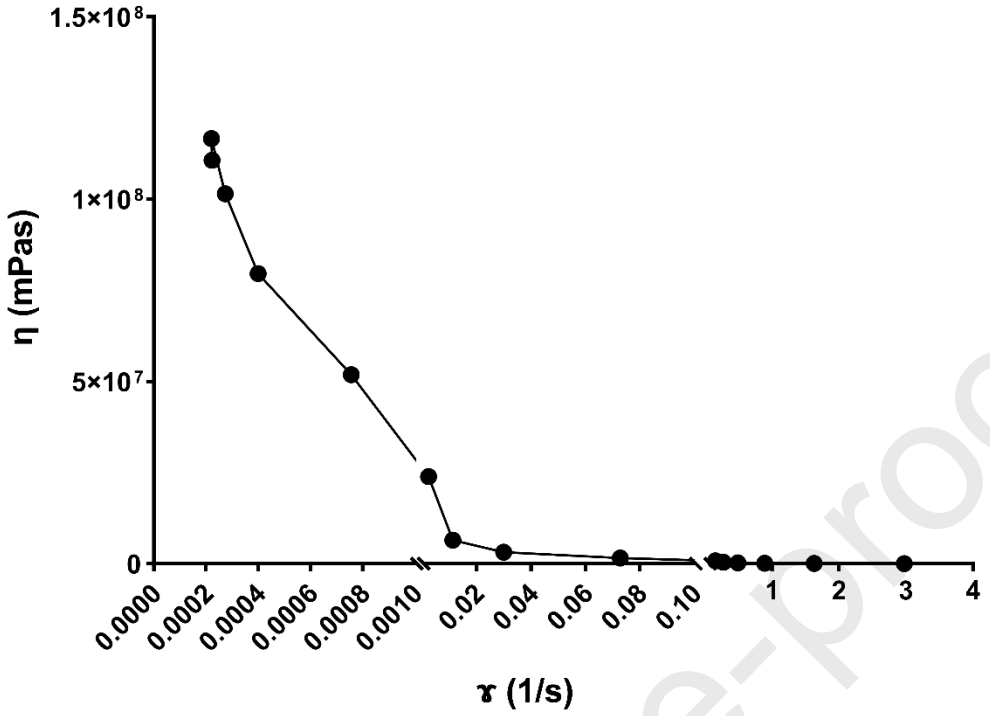

Figure 5. Rheogram of TAK-441 loaded TPGS micelle-based 3 % HPMC gel.

TAK-441 content in Formulation E and the HPMC gel of Formulation E packaged in aluminum tubes (Nussbaum Kesswil AG, Switzerland) was quantified at different time points for a period of 6 months (stored at 4 °C) using UHPLC-MS/MS (**Figure 6**). After 6 months, TAK-441 content in the micelle solution was 79.62% of the initial value, whereas in the micelle gel, TAK-441 content was 91.86% of the initial amount. The micelles were found to be intact in the gel formulation (**Supplementary Data, Section 6**).

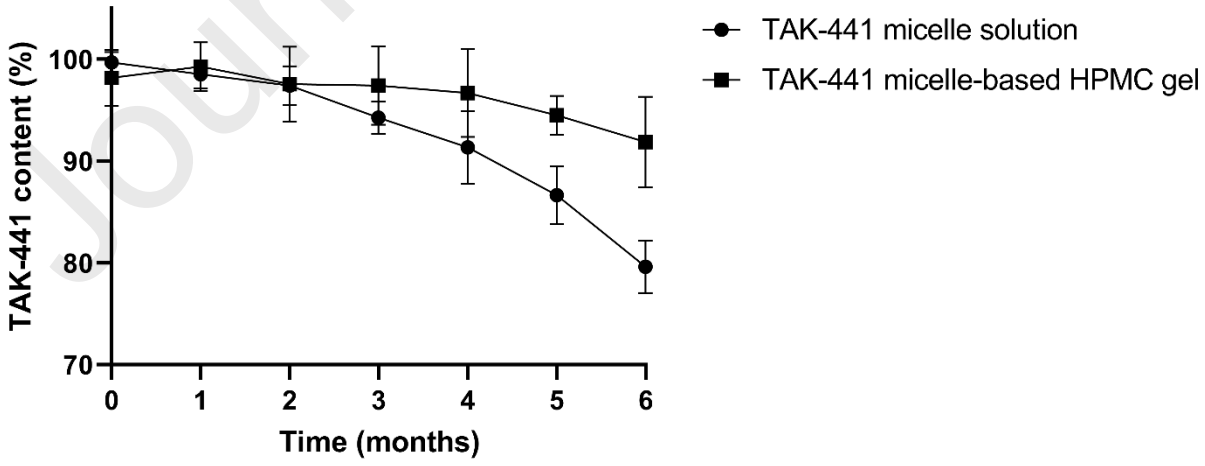

Figure 6. Stability of TAK-441 loaded micelle formulations

3.3.2 Determining the cutaneous delivery and biodistribution of TAK-441 from micelle-HPMC gel in human skin

As seen for the porcine skin experiments, the amounts of TAK-441 permeated across human skin were again below the LOD of the UHPLC-MS/MS method after an application time of 12 h. Greater skin deposition of TAK-441 was observed for the micelle-HPMC gel (**Figure 7A**): the amounts deposited from the micelle-HPMC gel and control HPMC gel formulations under infinite dose conditions were 1.17 ± 0.21 µg/cm^2 and 0.22 ± 0.07 µg/cm^2 (p=0.002, one-way ANOVA; n = 6) and the corresponding values for finite dosing were 0.40 ± 0.11 µg/cm^2 and 0.05 ± 0.02 µg/cm^2 (p=0.002, one-way ANOVA; n = 6), respectively. The cutaneous biodistribution under infinite and finite dose conditions revealed similar profiles to those observed in porcine skin. Greater amounts of TAK-441 were again present in the epidermal region (**Figure 7B and 7C**). For example, the estimated TAK-441 concentrations achieved on the 0-50 µm region, based on the amounts of TAK-441 delivered by micelle-HPMC gel at infinite and finite dose, were >22,000-fold and >7,800-fold higher than the IC_{50}, respectively; whereas, for the 50-100 µm region, the corresponding values were >9,400-fold and >3,100-fold higher, respectively.

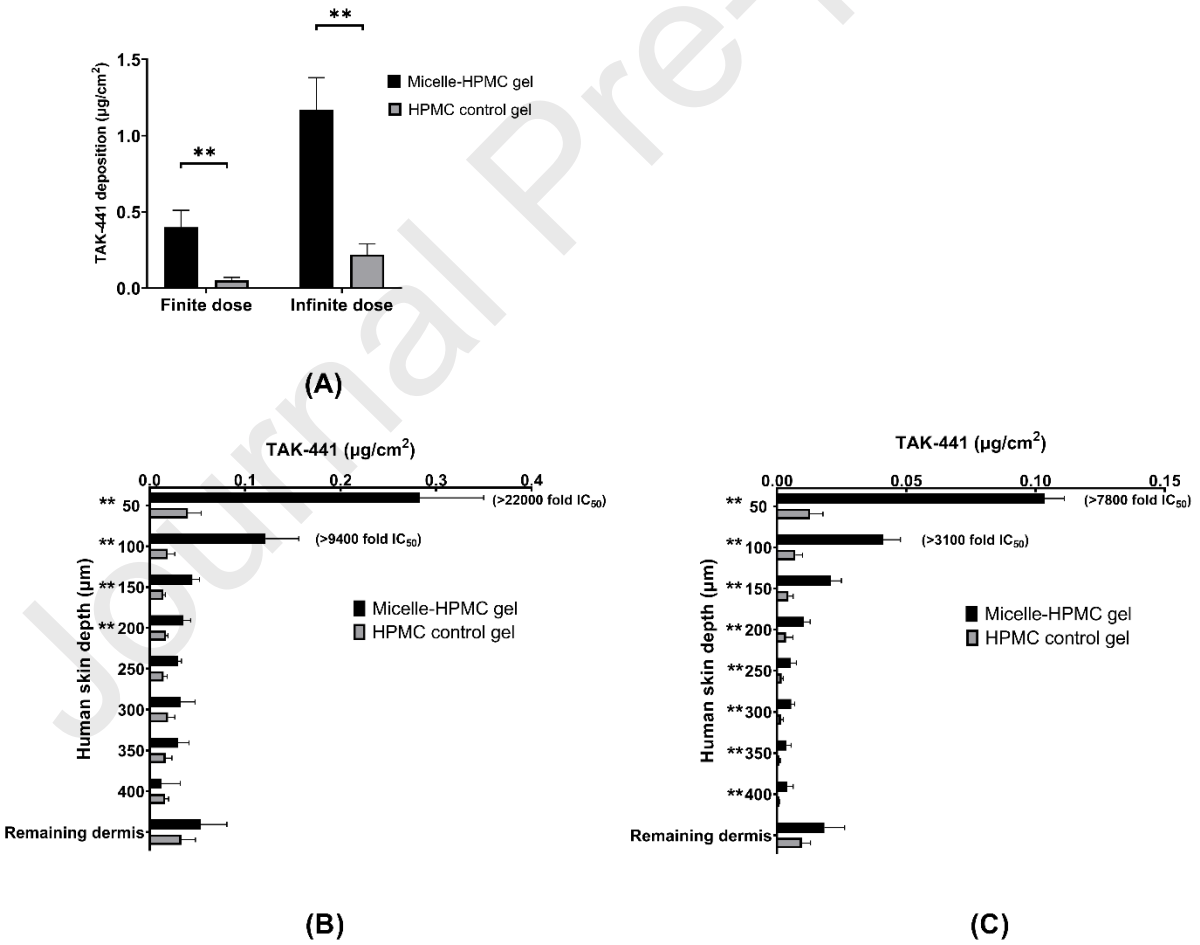

Figure 7. Cutaneous deposition and biodistribution of TAK-441 in human skin (micelle-based HPMC gel formulation, n = 6). **(A)** Cutaneous deposition of TAK-441, **(B)** Cutaneous biodistribution of TAK-441 at infinite dose, and **(C)** Cutaneous biodistribution of TAK-441 at finite dose; (**P < 0.05, one way ANOVA). (Mean ± SD)

The micelle-HPMC gel showed superiority over the HPMC control gel in all of the cutaneous delivery experiments performed. TAK-441 distribution in the HPMC gel is most likely more uniform than is the case for the micelle-HPMC formulation. TPGS micelles containing the TAK-441 in the lipophilic interior of the micelle, create a drug depot at the skin surface and, in particular, promote an accumulation of TAK-441 in the inter-cluster regions and the hair follicles (Kandekar et al., 2018; Lapteva et al., 2015, 2014b). The TPGS micelles may begin to disassemble upon coming into contact with the lipophilic stratum corneum, given the possibility to form different intermolecular interactions. This will release the "internalized" TAK-441 and make it available as a molecular dispersion. Another important factor affecting micelle stability and possible collapse will be water evaporation from the formulation on the skin surface. The effect of water loss, and the transformation/metamorphosis of the formulation, will be more important under finite dose conditions (Surber and Knie, 2018). Given its poor aqueous solubility, the release of TAK-441 from the micelles will result in local (super)saturation and the high thermodynamic activity will favor partitioning from the aqueous environment of the formulation and into the skin (Hadgraft, 1999; Moser et al., 2001; Schwarb et al., 1999; Cilurzo et al., 2015). The increased concentration of TAK-441 present in the stratum corneum results in an increased concentration gradient across the transport-limiting stratum corneum and hence an increased flux. This is manifest at a macroscopic level by the greater amounts of TAK-441 measured at each skin depth in the cutaneous biodistribution profile. Since nanocarriers have been shown to accumulate in and around hair follicles, the follicular pathway may play an enhanced role in the cutaneous penetration of TAK-441 and similar drugs applied using such delivery systems (Kandekar et al., 2018; Lapteva et al., 2015; Papakostas et al., 2011). It is also conceivable that the surfactant in the micelle formulation, can also act as a penetration enhancer; indeed, we have shown using MS imaging that TPGS can penetrate into the epidermis (Quartier et al., 2021a, 2021b).

4. Conclusion

The results obtained in this study confirmed that incorporation of TAK-441 in TPGS micelles was feasible and that the micelle-HPMC gel formulation of TAK-441 enabled its cutaneous delivery with the attainment of concentrations in the epidermal region that were orders of magnitude greater than the IC_{50} for inhibition of the HH pathway. Given that one of the factors limiting the use of HH inhibitors generally, and constraining the clinical development of TAK-441, is the incidence of adverse effects, it was important to note that the concentrations in the permeation samples were substantially lower than the LOD of the sensitive UHPLC-MS/MS method (<1.29 ng/mL corresponding to a cumulative permeation <0.1 pg/cm^2). This minimal permeation of TAK-441 across the skin should contribute to a reduction in the incidence of systemic side effects. It is clear that cutaneous delivery of TAK-441 from micelles to diseased human skin might be different to that observed in healthy tissue and dependent upon the type of the lesion and this would require further investigation *in vivo*.

5. Appendix list

Appendix 1: Supplementary Data

Appendix 2: Animated demonstration of microformulation technique

Declaration of competing interest

Vincent Ling is an employee of Takeda Pharmaceuticals, Cambridge, MA.

Acknowledgments

We thank the University of Geneva for a teaching assistantship for A.D. and financial support for M.L. TAK-441 was kindly provided by Takeda Pharmaceutical Company Ltd, Japan. We would also like to acknowledge it for providing financial support together with the Fondation Ernst and Lucie Schmidheiny for the purchase of the Waters Xevo TQ-MS detector. We also express our thanks to Professor Brigitte Pittet-Cuénod and her colleagues from the Department of Plastic, Aesthetic and Reconstructive Surgery, Geneva University Hospital (Geneva, Switzerland) for providing human skin samples.

References

Aggarwal, N., Goindi, S., Mehta, S.D., 2012. Preparation and Evaluation of Dermal Delivery System of Griseofulvin Containing Vitamin E-TPGS as Penetration Enhancer. AAPS PharmSciTech 13, 67–74. https://doi.org/10.1208/s12249-011-9722-y

Athar, M., Tang, X., Lee, J.L., Kopelovich, L., Kim, A.L., 2006. Hedgehog signalling in skin development and cancer. Exp. Dermatol. 15, 667–677. https://doi.org/10.1111/j.1600-0625.2006.00473.x

Bachhav, Y.G., Mondon, K., Kalia, Y.N., Gurny, R., Möller, M., 2011. Novel micelle formulations to increase cutaneous bioavailability of azole antifungals. J. Controlled Release 153, 126–132. https://doi.org/10.1016/j.jconrel.2011.03.003

Brummer, R., Godersky, S., 1999. Rheological studies to objectify sensations occurring when cosmetic emulsions are applied to the skin. Colloids Surf. Physicochem. Eng. Asp. 152, 89–94. https://doi.org/10.1016/S0927-7757(98)00626-8

Burness, C.B., 2015. Sonidegib: First Global Approval. Drugs 75, 1559–1566. https://doi.org/10.1007/s40265-015-0458-y

Cilurzo, F., Casiraghi, A., Selmin, F., Minghetti, P., 2015. Supersaturation as a tool for skin penetration enhancement. Curr. Pharm. Des. 21, 2733–2744. https://doi.org/10.2174/1381612821666150428125046

Couvé-Privat, S., Bouadjar, B., Avril, M.F., Sarasin, A., Daya-Grosjean, L., 2002. Significantly high levels of ultraviolet-specific mutations in the smoothened gene in basal cell carcinomas from DNA repair-deficient xeroderma pigmentosum patients. Cancer Res. 62, 7186–7189.

Dahmana, N., Mugnier, T., Gabriel, D., Favez, T., Kowalczuk, L., Behar-Cohen, F., Gurny, R., Kalia, Y.N., 2021. Polymeric micelle mediated follicular delivery of spironolactone: Targeting the mineralocorticoid receptor to prevent glucocorticoid-induced activation and delayed cutaneous wound healing. Int. J. Pharm. 604, 120773. https://doi.org/10.1016/j.ijpharm.2021.120773

Danial, C., Sarin, K.Y., Oro, A.E., Chang, A.L.S., 2016. An Investigator-Initiated Open-Label Trial of Sonidegib in Advanced Basal Cell Carcinoma Patients Resistant to Vismodegib. Clin. Cancer Res. Off. J. Am. Assoc. Cancer Res. 22, 1325–1329. https://doi.org/10.1158/1078-0432.CCR-15-1588

Daya-Grosjean, L., Sarasin, A., 2000. UV-specific mutations of the human patched gene in basal cell carcinomas from normal individuals and xeroderma pigmentosum patients. Mutat. Res. Mol. Mech. Mutagen. 450, 193–199. https://doi.org/10.1016/S0027-5107(00)00025-7

Dick, I.P., Scott, R.C., 1992. Pig ear skin as an in-vitro model for human skin permeability. J. Pharm. Pharmacol. 44, 640–645. https://doi.org/10.1111/j.2042-7158.1992.tb05485.x

Dlugosz, A., Agrawal, S., Kirkpatrick, P., 2012. Vismodegib. Nat. Rev. Drug Discov. 11, 437–438. https://doi.org/10.1038/nrd3753

Gailani, M.R., Bale, A.E., 1997. Developmental Genes and Cancer: Role of Patched in Basal Cell Carcinoma of the Skin. JNCI J. Natl. Cancer Inst. 89, 1103–1109. https://doi.org/10.1093/jnci/89.15.1103

Goldman, J., Eckhardt, S.G., Borad, M.J., Curtis, K.K., Hidalgo, M., Calvo, E., Ryan, D.P., Wirth, L.J., Parikh, A., Partyka, J., Faessel, H., Gangolli, E., Stewart, S., Rosen, L.S., Bowles, D.W., 2015. Phase I Dose-Escalation Trial of the Oral Investigational Hedgehog Signaling Pathway Inhibitor TAK-441 in Patients with Advanced Solid Tumors. Clin. Cancer Res. 21, 1002–1009. https://doi.org/10.1158/1078-0432.CCR-14-1234

Gou, S., Monod, M., Salomon, D., Kalia, Y.N., 2022. Simultaneous Delivery of Econazole, Terbinafine and Amorolfine with Improved Cutaneous Bioavailability: A Novel Micelle-Based Antifungal “Tri-Therapy.” Pharmaceutics 14, 271. https://doi.org/10.3390/pharmaceutics14020271

Gould, S.E., Low, J.A., Marsters, J.C., Robarge, K., Rubin, L.L., de Sauvage, F.J., Sutherlin, D.P., Wong, H., Yauch, R.L., 2014. Discovery and preclinical development of vismodegib. Expert Opin. Drug Discov. 9, 969–984. https://doi.org/10.1517/17460441.2014.920816

Greiderer, A., Steeneken, L., Aalbers, T., Vivó-Truyols, G., Schoenmakers, P., 2011. Characterization of hydroxypropylmethylcellulose (HPMC) using comprehensive two-dimensional liquid chromatography. J. Chromatogr. A 1218, 5787–5793. https://doi.org/10.1016/j.chroma.2011.04.076

Hadgraft, J., 1999. Passive enhancement strategies in topical and transdermal drug delivery. Int. J. Pharm. 184, 1–6. https://doi.org/10.1016/S0378-5173(99)00095-2

Herkenne, C., Naik, A., Kalia, Y.N., Hadgraft, J., Guy, R.H., 2006. Pig ear skin ex vivo as a model for in vivo dermatopharmacokinetic studies in man. Pharm. Res. 23, 1850–1856. https://doi.org/10.1007/s11095-006-9011-8

Ishii, T., Shimizu, Y., Nakashima, K., Kondo, S., Ogawa, K., Sasaki, S., Matsui, H., 2014. Inhibition mechanism exploration of investigational drug TAK-441 as inhibitor against Vismodegib-resistant Smoothened mutant. Eur. J. Pharmacol. 723, 305–313. https://doi.org/10.1016/j.ejphar.2013.11.014

Jacobi, U., Kaiser, M., Toll, R., Mangelsdorf, S., Audring, H., Otberg, N., Sterry, W., Lademann, J., 2007. Porcine ear skin: an in vitro model for human skin. Skin Res. Technol. 13, 19–24. https://doi.org/10.1111/j.1600-0846.2006.00179.x

Jain, S., Song, R., Xie, J., 2017. Sonidegib: mechanism of action, pharmacology, and clinical utility for advanced basal cell carcinomas. OncoTargets Ther. Volume 10, 1645–1653. https://doi.org/10.2147/OTT.S130910

Kalia, Y.N., Darade, A.R., 2022. Method for Preparing Nanosystems. EP4005557A1.

Kandekar, S.G., del Río-Sancho, S., Lapteva, M., Kalia, Y.N., 2018. Selective delivery of adapalene to the human hair follicle under finite dose conditions using polymeric micelle nanocarriers. Nanoscale 10, 1099–1110. https://doi.org/10.1039/C7NR07706H

Kandekar, S.G., Singhal, M., Sonaje, K.B., Kalia, Y.N., 2019. Polymeric micelle nanocarriers for targeted epidermal delivery of the hedgehog pathway inhibitor vismodegib: formulation development and cutaneous biodistribution in human skin. Expert Opin. Drug Deliv. 16, 667–674. https://doi.org/10.1080/17425247.2019.1609449

Kwak, M.-S., Ahn, H.-J., Song, K.-W., 2015. Rheological investigation of body cream and body lotion in actual application conditions. Korea-Aust. Rheol. J. 27, 241–251. https://doi.org/10.1007/s13367-015-0024-x

Lapteva, M., Mignot, M., Mondon, K., Möller, M., Gurny, R., Kalia, Y.N., 2019. Self-assembled mPEG-hexPLA polymeric nanocarriers for the targeted cutaneous delivery of imiquimod. Eur. J. Pharm. Biopharm. Off. J. Arbeitsgemeinschaft Pharm. Verfahrenstechnik EV 142, 553–562. https://doi.org/10.1016/j.ejpb.2019.01.008

Lapteva, M., Möller, M., Gurny, R., Kalia, Y.N., 2015. Self-assembled polymeric nanocarriers for the targeted delivery of retinoic acid to the hair follicle. Nanoscale 7, 18651–18662. https://doi.org/10.1039/C5NR04770F

Lapteva, M., Mondon, K., Möller, M., Gurny, R., Kalia, Y.N., 2014a. Polymeric Micelle Nanocarriers for the Cutaneous Delivery of Tacrolimus: A Targeted Approach for the Treatment of Psoriasis. Mol. Pharm. 11, 2989–3001. https://doi.org/10.1021/mp400639e

Lapteva, M., Santer, V., Mondon, K., Patmanidis, I., Chiriano, G., Scapozza, L., Gurny, R., Möller, M., Kalia, Y.N., 2014b. Targeted cutaneous delivery of ciclosporin A using micellar nanocarriers and the possible role of inter-cluster regions as molecular transport pathways. J. Controlled Release 196, 9–18. https://doi.org/10.1016/j.jconrel.2014.09.021

Lauressergues, E., Heusler, P., Lestienne, F., Troulier, D., Rauly-Lestienne, I., Tourette, A., Ailhaud, M., Cathala, C., Tardif, S., Denais-Lalième, D., Calmettes, M., Degryse, A., Dumoulin, A., De Vries, L., Cussac, D., 2016. Pharmacological evaluation of a series of smoothened antagonists in signaling pathways and after topical application in a depilated mouse model. Pharmacol. Res. Perspect. 4. https://doi.org/10.1002/prp2.214

Lavasanifar, A., Samuel, J., Kwon, G.S., 2002. Poly(ethylene oxide)-block-poly(l-amino acid) micelles for drug delivery. Adv. Drug Deliv. Rev. 54, 169–190. https://doi.org/10.1016/S0169-409X(02)00015-7

Madan, V., Lear, J.T., Szeimies, R.-M., 2010. Non-melanoma skin cancer 375, 13.

Moser, K., Kriwet, K., Froehlich, C., Kalia, Y.N., Guy, R.H., 2001. Supersaturation: enhancement of skin penetration and permeation of a lipophilic drug. Pharm. Res. 18, 1006–1011. https://doi.org/10.1023/a:1010948630296

Nguyen, N.M., Cho, J., 2022. Hedgehog Pathway Inhibitors as Targeted Cancer Therapy and Strategies to Overcome Drug Resistance. Int. J. Mol. Sci. 23, 1733. https://doi.org/10.3390/ijms23031733

Ohashi, T., Oguro, Y., Tanaka, T., Shiokawa, Z., Tanaka, Y., Shibata, S., Sato, Y., Yamakawa, H., Hattori, H., Yamamoto, Y., Kondo, S., Miyamoto, M., Nishihara, M., Ishimura, Y., Tojo, H., Baba, A., Sasaki, S., 2012. Discovery of the investigational drug TAK-441, a pyrrolo[3,2-c]pyridine derivative, as a highly potent and orally active hedgehog signaling inhibitor: Modification of the core skeleton for improved solubility. Bioorg. Med. Chem. 20, 5507–5517. https://doi.org/10.1016/j.bmc.2012.07.034

Papakostas, D., Rancan, F., Sterry, W., Blume-Peytavi, U., Vogt, A., 2011. Nanoparticles in dermatology. Arch. Dermatol. Res. 303, 533–550. https://doi.org/10.1007/s00403-011-1163-7

Papas, A.M., 2021. Chapter 59 - Vitamin E TPGS and its applications in nutraceuticals, in: Gupta, R.C., Lall, R., Srivastava, A. (Eds.), Nutraceuticals (Second Edition). Academic Press, pp. 991–1010. https://doi.org/10.1016/B978-0-12-821038-3.00059-8

Quartier, J., Lapteva, M., Boulaguiem, Y., Guerrier, S., Kalia, Y.N., 2021a. Polymeric micelle formulations for the cutaneous delivery of sirolimus: A new approach for the treatment of facial angiofibromas in tuberous sclerosis complex. Int. J. Pharm. 604, 120736. https://doi.org/10.1016/j.ijpharm.2021.120736

Quartier, J., Rao, W., Slade, S., Métral, F., Lapteva, M., Kalia, Y.N., 2021b. DESI-MS imaging to visualize spatial distribution of xenobiotics and endogenous lipids in the skin. Int. J. Pharm. 607, 120967. https://doi.org/10.1016/j.ijpharm.2021.120967

Robarge, K.D., Brunton, S.A., Castanedo, G.M., Cui, Y., Dina, M.S., Goldsmith, R., Gould, S.E., Guichert, O., Gunzner, J.L., Halladay, J., Jia, W., Khojasteh, C., Koehler, M.F.T., Kotkow, K., La, H., LaLonde, R.L., Lau, K., Lee, L., Marshall, D., Marsters, J.C., Murray, L.J., Qian, C., Rubin, L.L., Salphati, L., Stanley, M.S., Stibbard, J.H.A., Sutherlin, D.P., Ubhayaker, S., Wang, S., Wong, S., Xie, M., 2009. GDC-0449—A potent inhibitor of the hedgehog pathway. Bioorg. Med. Chem. Lett. 19, 5576–5581. https://doi.org/10.1016/j.bmcl.2009.08.049

Roewert-Huber, J., Lange-Asschenfeldt, B., Stockfleth, E., Kerl, H., 2007. Epidemiology and aetiology of basal cell carcinoma: Epidemiology and aetiology of BCC. Br. J. Dermatol. 157, 47–51. https://doi.org/10.1111/j.1365-2133.2007.08273.x

Samarasinghe, V., Madan, V., 2012. Nonmelanoma skin cancer. J. Cutan. Aesthetic Surg. 5, 3. https://doi.org/10.4103/0974-2077.94323

Schmook, F.P., Meingassner, J.G., Billich, A., 2001. Comparison of human skin or epidermis models with human and animal skin in in-vitro percutaneous absorption. Int. J. Pharm. 215, 51–56. https://doi.org/10.1016/s0378-5173(00)00665-7

Schwarb, F.P., Imanidis, G., Smith, E.W., Haigh, J.M., Surber, C., 1999. Effect of concentration and degree of saturation of topical fluocinonide formulations on in vitro membrane transport and in vivo availability on human skin. Pharm. Res. 16, 909–915. https://doi.org/10.1023/a:1018890422825

Staples, M.P., Elwood, M., Burton, R.C., Williams, J.L., Marks, R., Giles, G.G., 2006. Non-melanoma skin cancer in Australia: the 2002 national survey and trends since 1985. Med. J. Aust. 184, 6–10. https://doi.org/10.5694/j.1326-5377.2006.tb00086.x

Sugar-Based Surfactants, n.d.

Vadlapudi, A.D., Cholkar, K., Vadlapatla, R.K., Mitra, A.K., 2014. Aqueous Nanomicellar Formulation for Topical Delivery of Biotinylated Lipid Prodrug of Acyclovir: Formulation Development and Ocular Biocompatibility. J. Ocul. Pharmacol. Ther. 30, 49–58. https://doi.org/10.1089/jop.2013.0157

Yauch, R.L., Dijkgraaf, G.J.P., Alicke, B., Januario, T., Ahn, C.P., Holcomb, T., Pujara, K., Stinson, J., Callahan, C.A., Tang, T., Bazan, J.F., Kan, Z., Seshagiri, S., Hann, C.L., Gould, S.E., Low, J.A., Rudin, C.M., de Sauvage, F.J., 2009. Smoothened Mutation Confers Resistance to a Hedgehog Pathway Inhibitor in Medulloblastoma. Science 326, 572–574. https://doi.org/10.1126/science.1179386

Zhang, Z., Chu, Q., Wu, Y., Zhuang, X., Bao, Y., Wu, T., Tan, S., 2015. D-α-tocopherol polyethylene glycol succinate-based derivative nanoparticles as a novel carrier for paclitaxel delivery. Int. J. Nanomedicine 5219. https://doi.org/10.2147/IJN.S82847

Polymeric micelles for cutaneous delivery of the hedgehog pathway inhibitor TAK-441: formulation development and cutaneous biodistribution in porcine and human skin

Aditya R. Darade[a,b], Maria Lapteva[a,b], Vincent Ling[c], Yogeshvar N. Kalia[a,b*]

[a] School of Pharmaceutical Sciences, University of Geneva, CMU, 1 rue Michel-Servet, 1211, Geneva 4, Switzerland

[b] Institute of Pharmaceutical Sciences Western Switzerland, University of Geneva, Geneva, Switzerland

[c] Takeda Pharmaceuticals, Drug Delivery Technologies Search and Evaluation, 40 Landsdowne St, Cambridge MA 02139

CRediT authorship contribution statement

Aditya R. Darade: investigation, methodology, data curation, validation, manuscript writing — original draft, formal data analysis, generation of figures.

Maria Lapteva: investigation, methodology, writing – review & editing, supervision.

Vincent Ling: conceptualization and reviewing.

Yogeshvar N. Kalia: conceptualization, resources, data review, writing – review & editing, supervision, funding acquisition.

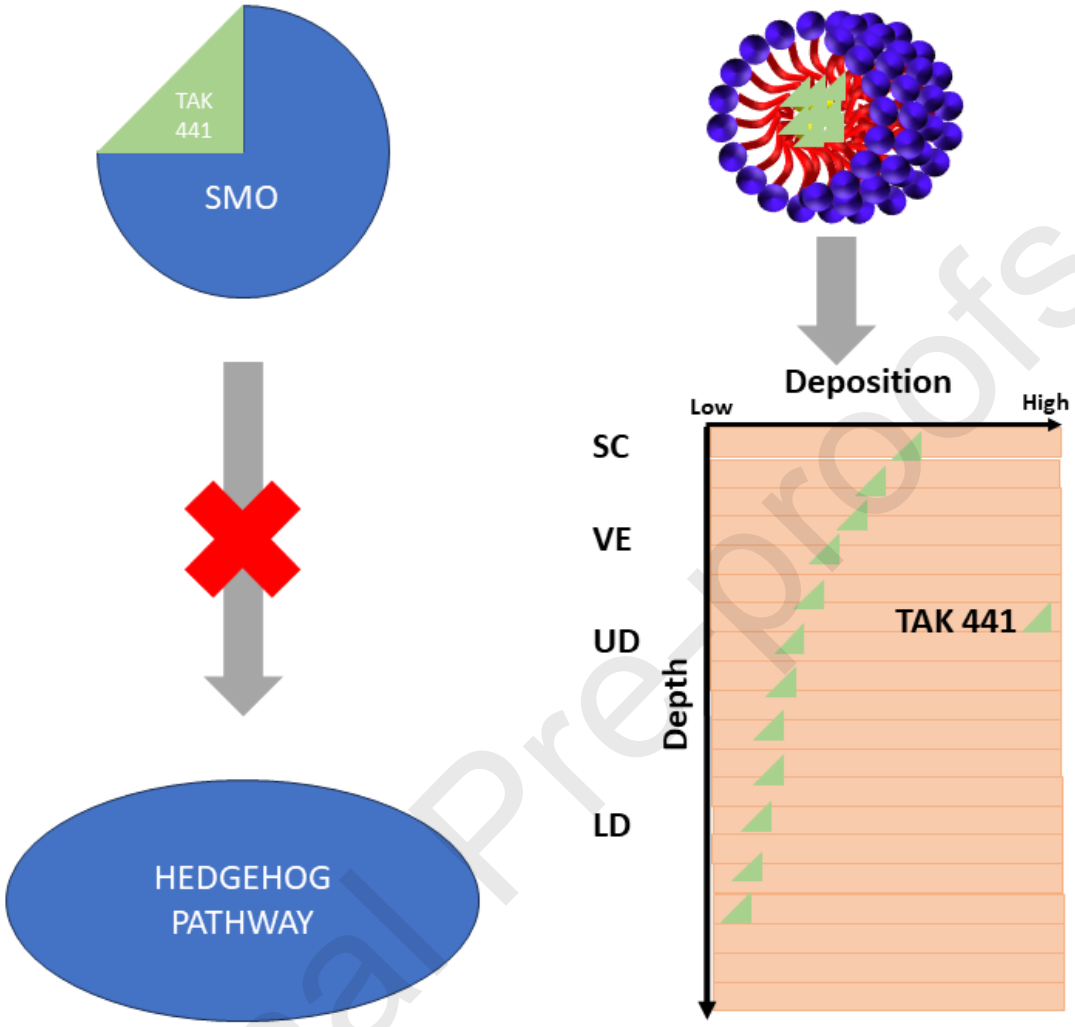

Declaration of interests

☐ The authors declare that they have no known competing financial interests or personal relationships that could have appeared to influence the work reported in this paper.

☒The authors declare the following financial interests/personal relationships which may be considered as potential competing interests:

Dr. Vincent Ling is an employee of Takeda Pharmaceuticals.